The Stoichiometry of $P2X_{2/6}$ Receptor Heteromers Depends on Relative Subunit Expression Levels

Nelson P. Barrera, Robert M. Henderson, Ruth D. Murrell-Lagnado, and J. Michael Edwardson
Department of Pharmacology, University of Cambridge, Cambridge CB2 1PD, United Kingdom

ABSTRACT Fast synaptic transmission involves the operation of ionotropic receptors, which are often composed of at least two types of subunit. We have developed a method, based on atomic force microscopy imaging to determine the stoichiometry and subunit arrangement within ionotropic receptors. We showed recently that the $P2X_2$ receptor for ATP is expressed as a trimer but that the $P2X_6$ subunit is unable to oligomerize. In this study we addressed the subunit stoichiometry of heteromers containing both $P2X_2$ and $P2X_6$ subunits. We transfected tsA 201 cells with both $P2X_2$ and $P2X_6$ subunits, bearing different epitope tags. We manipulated the transfection conditions so that either $P2X_2$ or $P2X_6$ was the predominant subunit expressed. By atomic force microscopy imaging of isolated receptors decorated with antiepitope antibodies, we demonstrate that when expression of the $P2X_2$ subunit predominates, the receptors contain primarily $2 \times P2X_2$ subunits and $1 \times P2X_6$ subunit. In contrast, when the $P2X_6$ subunit predominates, the subunit stoichiometry of the receptors is reversed. Our results show that the composition of P2X receptor heteromers is plastic and dependent on the relative subunit expression levels. We suggest that this property of receptor assembly might introduce an additional layer of subtlety into P2X receptor signaling.

INTRODUCTION

Ionotropic receptors, including members of the Cys-loop family (1), glutamate receptors (2), and P2X receptors for ATP (3), are often composed of more than one type of subunit. The subunit stoichiometry within a receptor can be variable and in some cases appears to depend on the relative subunit expression levels. For instance, distinct subunit stoichiometries of the $\alpha_4\beta_2$ nicotinic acetylcholine receptor have been produced both in *Xenopus* oocytes (4) and in human embryonic kidney cells (5) by variation in the ratios of complementary DNA (cDNA) for the α- and β-subunits. Receptors with these alternative subunit stoichiometries had different functional characteristics (4,5), indicating that plasticity in receptor assembly might be physiologically significant.

We have developed a method, based on atomic force microscopy (AFM) imaging, to determine the stoichiometry and subunit arrangement within ionotropic receptors. Epitope tags are engineered onto specific receptor subunits, and the receptors are expressed exogenously by transfection of tsA 201 cells. The receptors are isolated and decorated with antiepitope antibodies. The geometry of complexes between the receptor and the antibodies, as determined by AFM, then reveals the architecture of the receptor. We have used this method to demonstrate that α_1-subunits within a γ-aminobutyric acid A ($GABA_A$) receptor composed of $2 \times \alpha_1$-, $2 \times \beta_2$-, and $1 \times \gamma_2$-subunits are not adjacent but separated by another subunit (6). In addition, we have shown that the heteromeric $5\text{-}HT_3$ receptor, composed of A- and B-subunits, has a stoichiometry of 2A:3B and a subunit arrangement of B-B-A-B-A (7).

P2X receptors incorporate a cation-selective ion channel that is opened in response to ATP binding (3,8,9). Seven P2X receptor subunits have been identified, and these subunits associate together to form homo- or heterooligomeric receptors. Each subunit spans the membrane twice, and both N- and C-termini are intracellular. The large extracellular domain is glycosylated and contains several cysteine residues that form multiple disulfide bonds. Of the seven P2X receptor subunits, all but $P2X_7$ are able to form heteromers in combination with other subunits (10). In some cases, it is known that the functional properties of the heteromer are distinct from those of homomers composed of the constituent subunits (11–13).

We have shown previously by AFM analysis that the homomeric $P2X_2$ receptor is a trimer, whereas the $P2X_6$ receptor subunit cannot oligomerize by itself (14), although oligomerization can be induced by the introduction of charged residues into the N-terminal region (15). In this study, we set out to determine the architecture of receptors containing both $P2X_2$ and $P2X_6$ subunits. Despite its inability to form homomeric receptors, $P2X_6$ readily forms heteromers with $P2X_2$, producing receptors with properties different from those of the parent receptors. For example, the calcium permeability of the $P2X_{2/6}$ heteromer is significantly greater than that of the $P2X_2$ homomer (11), a difference that might have important implications in synaptic transmission. In support of this suggestion, $P2X_2$ and $P2X_6$ subunits have overlapping distributions in the central nervous system (16,17).

We transfected cells with mixtures of cDNA encoding the two subunits in ratios designed to produce a predominance of either the $P2X_2$ or the $P2X_6$ subunit. We then asked whether

Submitted November 14, 2006, and accepted for publication March 20, 2007.

Address reprint requests to Dr. J. Michael Edwardson, Dept. of Pharmacology, University of Cambridge, Tennis Court Road, Cambridge CB2 1PD, UK. Tel.: 44-1223-334014; Fax: 44-1223-334100; E-mail: jme1000@cam.ac.uk.

Editor: Richard W. Aldrich.

0006-3495/07/07/505/08 $2.00

doi: 10.1529/biophysj.106.101048

the receptor composition was affected by variation in the relative expression levels of the two subunits. We show that the subunit composition of the $P2X_{2/6}$ heteromer is indeed plastic, which likely has implications for cellular signaling through P2X receptors in vivo.

MATERIALS AND METHODS

Transient transfection of tsA 201 cells

cDNA encoding the rat $P2X_2$ receptor was subcloned into the pcDNA3.1/His vector (Invitrogen, Carlsbad, CA), which produces a protein tagged at its N-terminus with the His_6 epitope. The same $P2X_2$ receptor cDNA, bearing a hemagglutinin (HA) tag at its N-terminus and a FLAG tag in its extracellular loop, was subcloned into the pEGFP vector modified to remove the enhanced green fluorescent protein (EGFP) tag (Clontech, Palo Alto, CA). cDNA encoding the rat $P2X_6$ receptor, bearing either an HA or a His_6 tag at its C-terminus, was subcloned into the same modified pEGFP vector. Transient transfections of tsA 201 cells with $P2X_2$ and $P2X_6$ receptor DNA were carried out using the CalPhos mammalian transfection kit (Clontech), according to the manufacturer's instructions. For transfection of one 162-cm^2 culture flask, 30 μg of plasmid DNA was used. Relative amounts of $P2X_2$ and $P2X_6$ receptor DNA were varied to change the relative expression levels of the two subunits. For smaller numbers of cells (i.e., for the immunofluorescence experiments), amounts of DNA were scaled down appropriately. After transfection, cells were incubated for 24–48 h at 37°C to allow expression of the P2X receptors.

Solubilization and purification of His_6-tagged receptors

The procedure for the solubilization and purification of receptors was as described previously (6,7,14,15). Briefly, a crude membrane fraction prepared from transfected tsA 201 cells was solubilized in 1% (w/v) CHAPS (3-[(3-cholamidopropyl)dimethylammonio]-1-propanesulfonic acid), and the solubilized material was incubated with Ni^{2+}-agarose beads (Probond; Invitrogen, Carlsbad, CA). The beads were washed extensively, and bound protein was eluted with increasing concentrations of imidazole. Samples were analyzed by sodium dodecyl sulfate (SDS)-polyacrylamide gel electrophoresis, and protein was detected by immunoblotting, using mouse monoclonal antibodies against either the HA (Covance (Berkeley, CA) HA.11, 1:500) or the His_6 tag (Invitrogen; 1:500), as appropriate.

AFM imaging of receptors and receptor-antibody complexes

The methods for AFM imaging have been described in detail previously (6,7,14,15). The molecular volumes of the protein particles were determined from particle dimensions based on AFM images. After adsorption of the receptors onto the mica support, the particles adopt the shape of a spherical cap. The heights and half-height radii were measured from multiple cross sections of the same particle, and the molecular volume was calculated using the following equation,

$$V_m = (\pi h/6)(3r^2 + h^2), \quad (1)$$

where h is the particle height and r is the radius (18).

Molecular volume based on molecular weight was calculated using the equation

$$V_c = (M_0/N_0)(V_1 + dV_2), \quad (2)$$

where M_0 is the molecular mass, N_0 is Avogadro's number, V_1 and V_2 are the partial specific volumes of particle and water, respectively, and d is the extent of protein hydration (18).

RESULTS

Constructs were designed that, on transfection of tsA 201 cells, led to the expression of $P2X_2$ receptor subunits bearing either His_6 or HA epitope tags at their N-termini. Similarly, $P2X_6$ constructs produced subunits bearing either His_6 or HA tags (both C-terminal). Immunofluorescence, using appropriate monoclonal antiepitope antibodies, revealed the presence of the appropriately tagged receptors in cells transfected with cDNA encoding the single subunits (Fig. 1). When cells were transfected with combinations of one subunit tagged with His_6 and the other tagged with HA, immunofluorescence showed the expression of both tagged subunits. We have shown previously that the $P2X_2$ subunit forms homotrimers

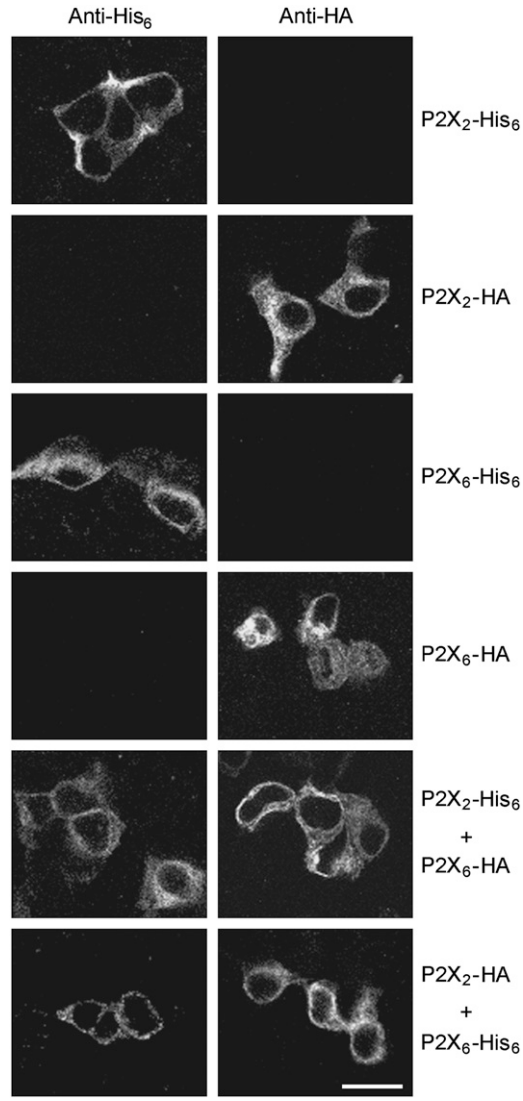

FIGURE 1 Immunofluorescence analysis of receptors. Cells were fixed with paraformaldehyde (4%), permeabilized with saponin, and incubated with appropriate monoclonal primary antibodies, followed by a Cy3-conjugated goat anti-mouse secondary antibody. Cells were imaged by confocal laser scanning microscopy. Scale bar, 20 μm.

(14) and is efficiently delivered to the cell surface (15,19). In contrast, the $P2X_6$ subunit cannot form homomeric receptors (14) and is retained in the endoplasmic reticulum (15). However, in the presence of $P2X_2$, $P2X_6$ is delivered to the cell surface, most likely in the form of $P2X_{2/6}$ heteromers (15).

Since the ability of available anti-His_6 antibodies to recognize their target epitope is sensitive to the location of the His_6 tag (i.e., whether the tag is N- or C-terminal), we used an anti-HA antibody that detects its epitope at any position in the tagged protein to determine the relative expression levels of the two subunits at different cDNA ratios. In a single experiment, we transfected cells with cDNA, encoding either $P2X_2$-HA plus $P2X_6$-His_6 or $P2X_2$-His_6 plus $P2X_6$-HA, at the same DNA ratios. We then prepared a crude membrane fraction from each population of cells and subjected equivalent amounts of each to SDS-polyacrylamide gel electrophoresis and immunoblotting using the anti-HA antibody. As can be seen from Fig. 2 *A*, the anti-HA antibody detected a doublet of molecular mass 70/64 kDa corresponding to the $P2X_2$ subunit and a single band of molecular mass 52 kDa corresponding to the $P2X_6$ subunit. The doublet given by the $P2X_2$ subunit likely represents completely and incompletely glycosylated forms of the protein, respectively. In addition to detecting the HA-tagged receptor subunits, the antibody also reacted with a nonspecific band running at a molecular mass of 60 kDa, which was present in all lanes. Note that no nonspecific labeling was seen when the same antibody was used for immunofluorescence (Fig. 1). When equal amounts of cDNA for the two subunits were used, the expression of the $P2X_2$ subunit was clearly greater than that of the $P2X_6$ subunit (Fig. 2 *A*, *left*). Densitometry of bands from three separate experiments indicated that the mean ratio of $P2X_2$/$P2X_6$ expression was 4.1:1. In contrast, when we used a cDNA ratio for $P2X_2$/$P2X_6$ of 1:4, the ratio of protein expression was 1:2.5 (Fig. 2 *A*, *right*).

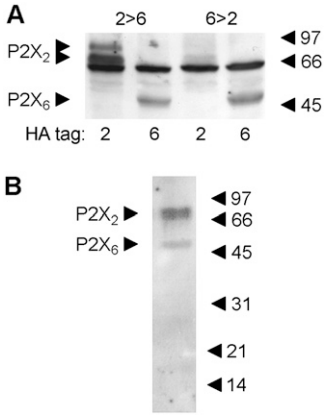

FIGURE 2 Immunoblot analysis of $P2X_{2/6}$ receptors. (*A*) Detection of receptors in crude membrane fractions of tsA 201 cells. Cells were transfected with cDNA encoding either $P2X_2$-HA plus $P2X_6$-His_6 or $P2X_2$-His_6 plus $P2X_6$-HA, at the same DNA ratios (1:1 $P2X_2$/$P2X_6$ for the *left two lanes* and 1:4 $P2X_2$/$P2X_6$ for the *right two lanes*). A crude membrane fraction was then prepared from each population of cells, and an equivalent amount of each fraction was subjected to SDS-polyacrylamide gel electrophoresis and immunoblotting using the anti-HA antibody followed by a horseradish peroxidase-conjugated goat anti-mouse secondary antibody. Immunoreactive bands were visualized using enhanced chemiluminescence. The positions of the $P2X_2$ (70/64 kDa) and the $P2X_6$ subunit (52 kDa) are indicated on the left. Note the presence of a nonspecific band running at 60 kDa in all lanes. The positions of molecular mass markers (kDa) are indicated on the right. (*B*) Detection of receptors in eluates from Ni^{2+}-agarose columns. $P2X_2$-His_6>$P2X_6$-HA receptors were immunoblotted with a mixture of anti-His_6 and anti-HA antibodies.

The crude membrane fractions prepared from cells transfected as described above were solubilized, and receptors were isolated through the binding of the His_6 tag, present on one of the two subunits, to Ni^{2+}-agarose beads. Receptors were eluted from the beads by treatment with imidazole. Fig. 2 *B* shows an immunoblot of $P2X_2$-His_6>$P2X_6$-HA receptors with a mixture of anti-HA and anti-His_6 antibodies. Three bands can be seen—a doublet at molecular mass of 70/64 kDa ($P2X_2$) and single band at 52 kDa ($P2X_6$). Note that the nonspecific band detected in the crude membrane fractions (Fig. 2 *A*) is no longer present.

AFM images of samples prepared from mock-transfected cells were almost featureless (Fig. 3 *A*). In contrast, images of isolated receptors showed clear populations of particles. We are therefore confident that the vast majority of these particles represent receptors. Fig. 3 *B* shows a typical image given by heteromeric ($P2X_2$-His_6>$P2X_6$-HA) receptors. As can be seen, the population of particles is heterogeneous in size. When the molecular volumes of a number of particles were determined and a frequency distribution produced, three clear peaks emerged, at 115 nm^3, 217 nm^3, and 360 nm^3 (Fig. 3 *C*; Table 1). Each particle shown in Fig. 3 *B* can be assigned on the basis of its size to one of the three peaks in the distribution. Clearly, the larger two peaks in the frequency distribution are approximately double and triple the volume of the smallest peak, suggesting that the peaks correspond to monomers, dimers, and trimers. We have previously calculated that the expected volume of a $P2X_2$ homotrimer—based on a molecular mass of 70 kDa, consisting of 55 kDa of core protein and 15 kDa of attached oligosaccharide—is 389 nm^3 (14). The expected volume would be ~360 nm^3 for a $P2X_{2/6}$ heteromer containing one $P2X_6$ subunit and ~320 nm^3 for a heteromer containing two $P2X_6$ subunits. These values would all be increased somewhat by the likely presence of detergent bound to the transmembrane regions of the isolated receptors. Given the various assumptions involved in these calculations, the volume determined for the third peak (360 nm^3) agrees well with the predicted volume, supporting the suggestion that this peak represents the trimeric form of the receptor.

Clear peaks corresponding to monomers, dimers, and trimers were not seen previously when we imaged $P2X_2$ and $P2X_6$ subunits alone (14). $P2X_2$ gave a single population of trimers, whereas $P2X_6$ behaved exclusively as monomers. When charged residues were introduced into the N-terminus

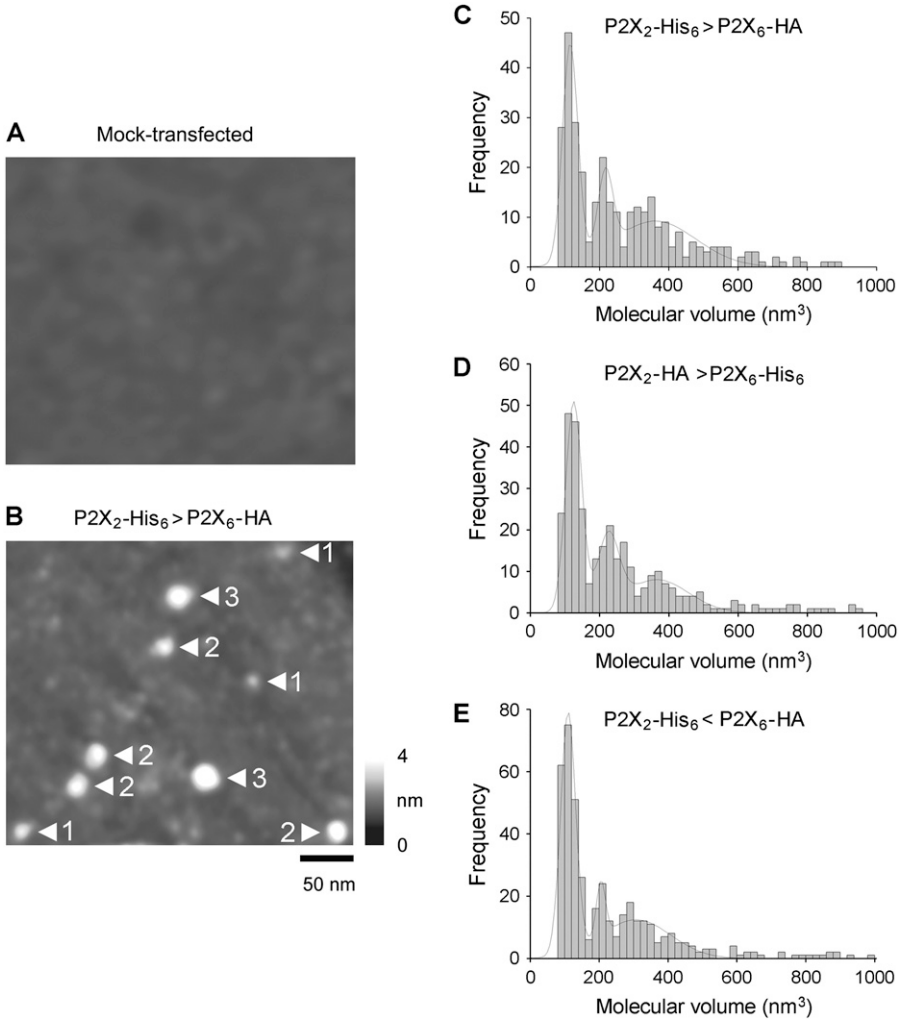

FIGURE 3 AFM imaging of $P2X_{2/6}$ receptors. (*A*) AFM image of a sample prepared from mock-transfected cells. (*B*) AFM image of a typical sample of $P2X_2$-His_6>$P2X_6$-HA receptors. Numbers 1, 2, and 3 indicate the assignment of the various particles into one of the three peaks in the frequency distribution of molecular volumes. A shade-height scale is shown at the right. (*C–E*) Frequency distributions of molecular volumes of $P2X_2$-His_6>$P2X_6$-HA (*C*), $P2X_2$-HA>$P2X_6$-His_6 (*D*), and $P2X_2$-His_6<$P2X_6$-HA (*E*) receptors. The curves indicate fitted Gaussian functions.

of the $P2X_6$ subunit, a mixture of trimers and monomers was produced, but there was no evidence of dimers (15). The presence of monomers, dimers, and trimers in these experiments suggests either that assembly intermediates are being isolated, which was not the case when $P2X_2$ homomers were studied previously (14) or, perhaps more likely, that the $P2X_{2/6}$ heteromers are less stable that the $P2X_2$ homomers and tend to fall apart during isolation. If the former explanation is correct, then only the His_6-tagged subunit (i.e., $P2X_2$) should be present in the smallest peak, whereas if the latter explanation is correct, then the smallest peak could contain both $P2X_2$ and $P2X_6$ subunits. When $P2X_2$-HA>$P2X_6$-His_6 receptors were expressed (i.e., the epitope tags on the two subunits were switched around but the ratio of subunit expression remained the same), the three peaks in the molecular volume distribution were again seen, and the sizes of the peaks were very similar to those described above—124 nm^3, 224 nm^3, and 365 nm^3 (Fig. 3 *D*; Table 1). Interestingly, when $P2X_2$-His_6<$P2X_6$-HA receptors were expressed (i.e., the subunit expression ratio was reversed to generate an excess of the smaller $P2X_6$ subunit), the sizes of all three peaks were reduced, to 110 nm^3, 205 nm^3, and 307 nm^3 (Fig. 3 *E*; Table 1). This result suggests that the receptors are indeed tending to fall apart during isolation and also that more $P2X_6$ subunits might be incorporated into the trimers at a higher ratio of $P2X_6$ expression. Note that the proportion of the particles assigned to the trimeric peak (~⅓ of the total) was similar for all three receptor compositions (Table 1).

TABLE 1 Molecular volumes of the P2X receptors

	Molecular volume ± SE (nm^3)		
Subunit expression	Peak 1	Peak 2	Peak 3
$P2X_2$-His_6 > $P2X_6$-HA	115 ± 2 (n = 125)	217 ± 3 (n = 65)	360 ± 13 (n = 121)
$P2X_2$-HA > $P2X_6$-His_6	124 ± 2 (n = 148)	224 ± 3 (n = 95)	365 ± 30 (n = 94)
$P2X_2$-His_6 < $P2X_6$-HA	110 ± 1 (n = 217)	205 ± 3 (n = 62)	307 ± 15 (n = 133)

Receptors were incubated with antiepitope antibodies, and the resulting receptor-antibody complexes were visualized by

AFM. As shown in Fig. 4 *A*, the $P2X_2$-His_6>$P2X_6$-HA receptor alone appeared as a heterogeneous spread of particles. Anti-HA samples showed a population of small particles, as expected. Samples resulting from coincubations of receptors and antibodies appeared very heterogeneous. Nevertheless, there were examples of large particles (components of the largest of three molecular volume peaks illustrated in Fig. 3) that were decorated by one (*arrows*) or two (*arrowheads*) smaller particles (presumably antibodies). Fig. 4 *B* shows galleries of images of individual receptors (trimers) either undecorated or decorated with either one or two antibodies. Similar features were seen irrespective of whether the antibody was directed against the His_6 or the HA tag. For each incubation condition, many data sets were analyzed and the status (i.e., undecorated or singly or double decorated) of a large number of trimeric particles was assessed (Table 2). To ensure that the apparent receptor-antibody complexes were genuine and not simply a consequence of large and small particles settling close together on the mica surface, two control experiments were carried out. In one control experiment, the antibody was not included. In this case a maximum of 1.2% of the particles appeared to have one small particle attached, and in only one case did there appear to be two small particles attached to one large particle. In the second control experiment, a His_6-tagged $P2X_2$ receptor homomer was incubated with an anti-HA antibody. In this case, only 0.9% of the large particles appeared to have one small particle attached, and there were no instances of a large particle appearing to be doubly decorated by small particles. In contrast to these results, when heteromeric receptors were incubated with antibodies against the epitope tags, a substantial proportion (24.7–36.1%) of the large particles were decorated by single antibodies, and up to 5.4% had two antibodies attached.

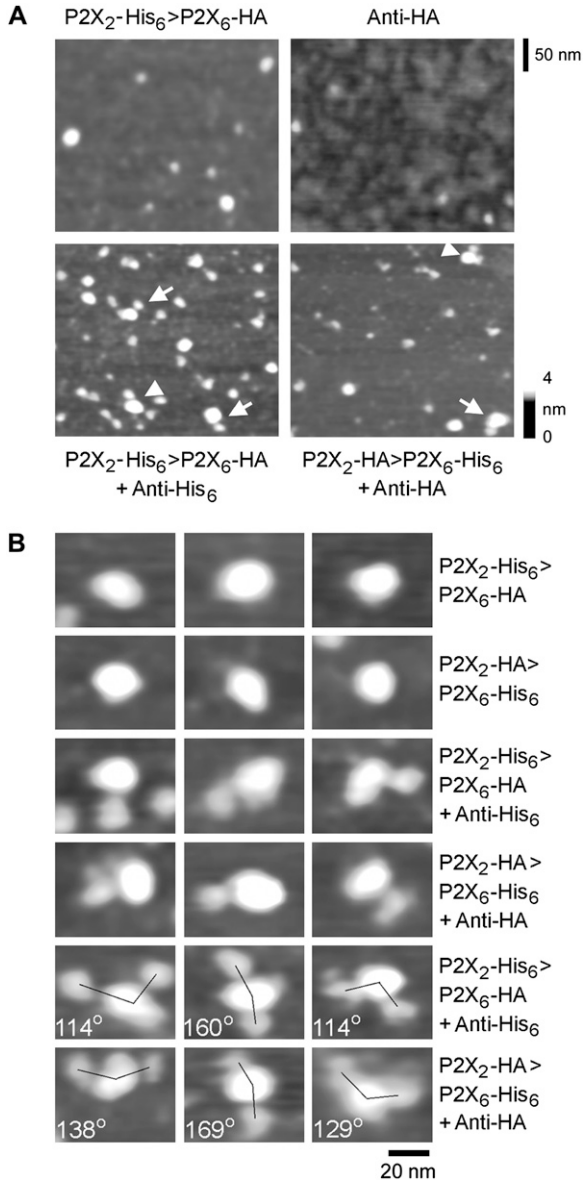

FIGURE 4 AFM imaging of complexes between $P2X_{2/6}$ receptors and anti-His_6 and anti-HA antibodies. (*A*) Images of $P2X_2$-His_6>$P2X_6$-HA receptors (*top left panel*), anti-HA antibodies (*top right panel*), and receptor-antibody complexes (*bottom panels*). Arrows indicate singly decorated receptors; arrowheads indicate doubly decorated receptors. A shade-height scale is shown at the right. (*B*) Zoomed images of receptors that are uncomplexed (*top two rows*) or bound by one (*middle two rows*) or two (*bottom two rows*) antibodies.

When $P2X_2$-His_6>$P2X_6$-HA receptors were expressed, 5.4% of the receptors were decorated by two anti-His_6 antibodies, and only 1.0% were decorated by two anti-HA antibodies (Table 2). This result, taken alone, indicates that 5.4 times more receptors contained two $P2X_2$ subunits than two $P2X_6$ subunits, under circumstances where the cells expressed 4.1 times as many $P2X_2$ subunits as $P2X_6$ subunits. In other words, the receptor composition approximately reflected the relative subunit expression. A potential complication with this interpretation is that if there was an excess of $P2X_2$ subunits over $P2X_6$ subunits, homomeric $P2X_2$ receptors might have been produced that would have been tagged with His_6 and therefore liable to be isolated along with the $P2X_{2/6}$ heteromers. To assess the significance of this complication, we repeated the experiment with $P2X_2$-HA>$P2X_6$-His_6 receptors. Now if $P2X_2$ homomers were present they should no longer be isolated. It is unlikely that there were significant numbers of $P2X_6$ homomers, since the $P2X_2$ subunits were in excess, and in addition, we have shown previously that $P2X_6$ does not oligomerize by itself (14). When the receptor decoration profiles were analyzed, it was found that 1.2% of the receptors were decorated by two anti-His_6 antibodies, whereas 4.6% were decorated by two anti-HA antibodies. This result indicates that 3.8 times more receptors contained two $P2X_2$ subunits than two $P2X_6$ subunits. This ratio is close to the one obtained before the tags were switched (5.4:1; above) and also to the ratio of subunit expression (4.1:1; Fig. 2 *A*). We conclude, therefore, that the presence of $P2X_2$ homomers has an insignificant impact on the result. Note also that the sizes of the largest molecular volume peaks for $P2X_2$-His_6>$P2X_6$-HA and $P2X_2$-HA>$P2X_6$-His_6 receptors were 360 and 365 nm^3, respectively. Both of these volumes are smaller than the

TABLE 2 Antibody tagging profile of the P2X receptors

Subunit expression	Number of particles bound to receptor	Receptor alone	%	Receptor plus anti-His_6 Ab	%	Receptors plus anti-HA Ab	%
$P2X_2$-His_6 >	0	311	99.4	692	58.4	513	74.3
$P2X_6$-HA	1	2	0.6	428	36.1	171	24.7
	2	0	0.0	64	5.4	7	1.0
	3	0	0.0	1	0.1	0	0.0
$P2X_2$-HA >	0	337	98.8	322	65.5	712	67.8
$P2X_6$-His_6	1	3	0.9	164	33.3	287	27.4
	2	1	0.3	6	1.2	48	4.6
	3	0	0.0	0	0.0	2	0.2
$P2X_2$-His_6 <	0	412	98.8	552	72.3	654	68.8
$P2X_6$-HA	1	5	1.2	198	25.9	249	26.2
	2	0	0.0	13	1.7	47	4.9
	3	0	0.0	1	0.1	1	0.1
$P2X_2$-His_6	0	-	-	-	-	629	99.1
	1	-	-	-	-	6	0.9
	2	-	-	-	-	0	0.0
	3	-	-	-	-	0	0.0

volume of 409 nm^3 obtained previously for the $P2X_2$ homomer (14), supporting the argument that no significant population of $P2X_2$ homomers is present when both $P2X_2$ and $P2X_6$ subunits are expressed.

Next, we switched around the expression levels of the two subunits and produced ($P2X_2$-His_6<$P2X_6$-HA) receptors. Now we found that 1.7% of the receptors were decorated by two anti-His_6 antibodies, whereas 4.9% were decorated by two anti-HA antibodies. In other words there were now 2.9 times as many receptors containing two $P2X_6$ subunits as those containing two $P2X_2$ subunits, under circumstances where there were 2.5 times as many $P2X_6$ subunits expressed as $P2X_2$ subunits (Fig. 2 *A*). As explained above, under these conditions, where $P2X_6$ subunits are in excess, it is unlikely that there are significant populations of either $P2X_2$ or $P2X_6$ homomers. Taken together, these results indicate that the subunit stoichiometry of the receptors depends on the relative expression levels of the subunits.

We have shown previously that $P2X_2$ receptor homomers are trimeric (14), and the frequency distribution of the $P2X_{2/6}$ heteromers reported here indicates that the largest molecular volume peak represents trimers. To confirm the stoichiometry of the heteromeric receptors, we measured the angles between antibodies in all cases of double decoration for the three conditions described above. As shown in Fig. 5, in all three cases the angle distribution had a peak at ~120° (116° ± 4° ($n = 64$) for $P2X_2$-His_6>$P2X_6$-HA receptors; 115° ± 5° ($n = 48$) for $P2X_2$-HA>$P2X_6$-His_6 receptors; and 119° ± 5° ($n = 47$) for $P2X_2$-His_6<$P2X_6$-HA receptors). These results strongly support our suggestion that the heteromers are indeed trimers.

DISCUSSION

In this study, we have used AFM imaging of antibody-decorated receptors to show that the stoichiometry of the $P2X_{2/6}$ heteromer depends on the relative expression levels of the two subunits. In the past, we have successfully used this approach to investigate the architecture of $GABA_A$ receptors (6), 5-HT_3 receptors (7), and other P2X receptors (14,15). It has been known for some time that heteromeric P2X receptors have different properties from those of homomers composed of the constituent monomers. For instance, the Hill slopes for agonist activation of $P2X_2$ and $P2X_3$ homomers are significantly higher than that of the $P2X_{2/3}$ heteromer, indicating a likely difference in the numbers of agonist binding sites on the homomeric and heteromeric receptors (12). Similarly, the $P2X_6$ subunit can increase the calcium permeability of the $P2X_2$ receptor (11) and change its pattern of modulation by pH (13). We have shown previously that when expressed alone, the $P2X_6$ subunit does not oligomerize to form functional receptors (14), and the monomers are retained in the endoplasmic reticulum (15). These observations suggest that the $P2X_6$ subunit acts as a versatile modulatory subunit rather than a functional receptor in its own right, an idea supported by the overlapping distributions of the $P2X_6$ subunit with both $P2X_2$ and $P2X_4$ subunits in the central nervous system (16,17,20,21). According to this scenario, the retention of the $P2X_6$ subunit in the endoplasmic reticulum might serve to provide an intracellular pool of subunits ready to be incorporated into heteromeric receptors. Our results here raise the possibility of yet another layer of subtlety in the operation of P2X receptors.

The plasticity of assembly of $P2X_{2/6}$ heteromers is similar to the behavior of the $\alpha_4\beta_2$ nicotinic acetylcholine receptor in which the subunit stoichiometry again seems to be determined by the relative subunit expression levels (4,5). For other members of the pentameric ionotropic receptor family, however, the subunit arrangement within the receptor rosette appears to be more firmly fixed. For example, there is general agreement that the arrangement of subunits within

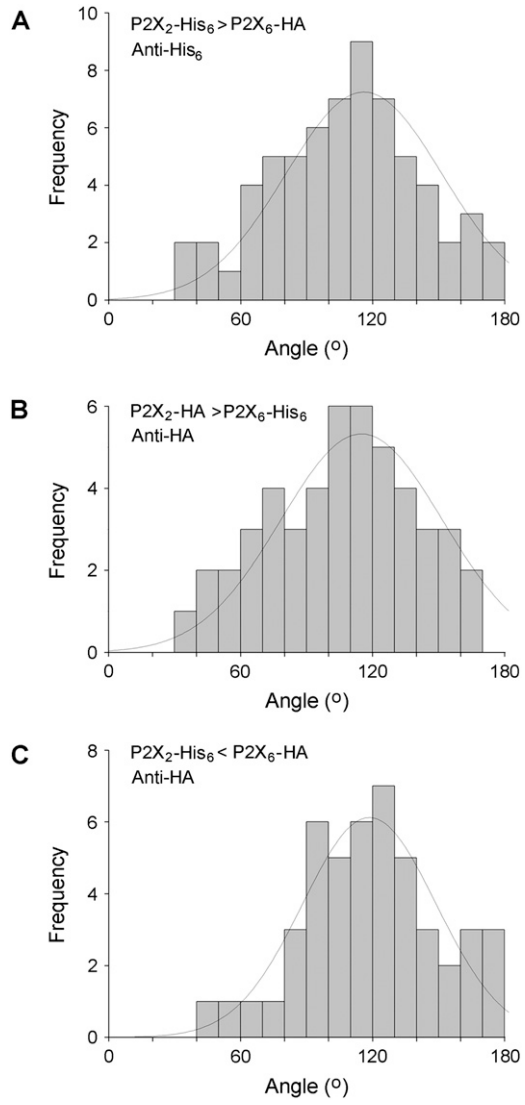

FIGURE 5 Frequency distributions of angles between antibodies for doubly decorated $P2X_{2/6}$ receptors. (*A*) $P2X_2$-His_6>$P2X_6$-HA receptors, anti-His_6 antibody. (*B*) $P2X_2$-HA>$P2X_6$-His_6 receptors, anti-HA antibody. (*C*) $P2X_2$-His_6<$P2X_6$-HA receptors, anti-His_6 antibody. The curves indicate fitted Gaussian functions.

the *Torpedo* electroplaque nicotinic acetylcholine receptor is $\alpha, \gamma, \alpha, \delta, \beta$ when viewed counterclockwise from the outside of the cell (22). Similarly, although functional $GABA_A$ receptors can be built from α_1- and β_2-subunits alone (23), when α_1-, β_2-, and γ_2-subunits are all expressed together, there appears to be only one way in which a functional receptor can be built, that is in the arrangement γ_2, β_2, α_1, β_2, α_1, when viewed counterclockwise from the outside of the cell (24). Finally, when we examined the subunit arrangement within the $5\text{-}HT_{3A/B}$ receptor in a previous study, we found a single arrangement, B-B-A-B-A, and no evidence for the presence of receptors with only two B-subunits (7). Even in the case of the $P2X_{2/3}$ heteromer, there appeared to be only one subunit stoichiometry ($1 \times P2X_2/2 \times P2X_3$) when approximately equal numbers of the subunits were expressed (12). Whether variations in the subunit arrangements within these other receptors might occur under circumstances of extreme variations in relative expression levels remains to be determined.

The assembly of P2X receptors has been studied previously by a series of elegant experiments using blue native gel electrophoresis and cross-linking strategies (25,26). One of these studies addressed the assembly of a $P2X_{1/2}$ heteromer (25), and some interesting findings emerged that are probably relevant to our own results. First, it appeared that the subunits preferentially formed heteromers, rather than homomers. Our evidence also indicates that only a very small number of $P2X_2$ homomers are produced, even when the $P2X_2$ subunit is in a fourfold excess over the $P2X_6$ subunit. Second, it was found that the $P2X_{1/2}$ heteromer was less stable than the $P2X_2$ homomer. For instance, the $P2X_2$ homomer was stable to treatment with 0.1 M dithiothreitol and only broke down into dimers and monomers in the presence of 8 M urea. In contrast, the $P2X_{1/2}$ heteromer was extensively dissociated by dithiothreitol. This result might reflect our own finding that the $P2X_{2/6}$ heteromers behaved as mixtures of monomers, dimers, and trimers, whereas we had previously found that the $P2X_2$ homomer behaves as a single population of trimers (14). Finally, when the $P2X_{1/2}$ heteromer dissociated, only a single species of dimer, composed of one $P2X_1$ subunit and one $P2X_2$ subunit, was produced. This finding might indicate that the affinity of the two different monomers for each other was greater than the affinities of identical monomers for each other. If a similar situation exists in our experiments, an assembly process can be envisaged that begins with a favored interaction between a $P2X_2$ subunit and a $P2X_6$ subunit, followed by a second interaction of the resulting heterodimer with either a $P2X_2$ or a $P2X_6$ monomer. The two monomers might then undergo mass-action competition with each other for entry into the complete receptor trimer. In this way, the receptor stoichiometry would reflect the relative amounts of the two subunits present at the site of assembly (presumably the endoplasmic reticulum).

We have shown here that the subunit stoichiometry of the heteromeric $P2X_{2/6}$ receptor is determined by the relative expression levels of the two subunits. We suggest that since the $P2X_6$ subunit is upregulated under pathological conditions such as cancer and zinc deficiency (27–30), this plasticity of receptor assembly is likely to have significant functional consequences.

This work was supported by a grant from the Biotechnology and Biological Sciences Research Council (B19797) to J.M.E. and R.M.H.

REFERENCES

1. Lester, H. A., M. I. Dibas, D. S. Dahan, J. F. Leite, and D. A. Dougherty. 2004. Cys-loop receptors: new twists and turns. *Trends Neurosci.* 27:329–336.

2. Furukawa, H., S. K. Singh, R. Mancusso, and E. Gouaux. 2005. Subunit arrangement and function in NMDA receptors. *Nature*. 438: 185–192.

3. North, R. A. 2002. Molecular physiology of P2X receptors. *Physiol. Rev*. 82:1013–1067.

4. Zwart, R., and H. P. M. Vijverberg. 1998. Four pharmacologically distinct subtypes of $\alpha4\beta2$ nicotinic acetylcholine receptor expressed in *Xenopus laevis* oocytes. *Mol. Pharmacol*. 54:1124–1131.

5. Nelson, M. E., A. Kuryatov, C. H. Choi, Y. Zhou, and J. Lindstrom. 2003. Alternate stoichiometries of $\alpha4\beta2$ nicotinic acetylcholine receptors. *Mol. Pharmacol*. 63:332–341.

6. Neish, C. S., I. L. Martin, M. Davies, R. M. Henderson, and J. M. Edwardson. 2003. Atomic force microscopy of ionotropic receptors bearing subunit-specific tags provides a method for determining receptor architecture. *Nanotechnology*. 14:864–872.

7. Barrera, N. P., P. Herbert, R. M. Henderson, I. L. Martin, and J. M. Edwardson. 2005. Atomic force microscopy reveals the stoichiometry and subunit arrangement of 5-HT_3 receptors. *Proc. Natl. Acad. Sci. USA*. 102:12595–12600.

8. Khakh, B. S. 2001. Molecular physiology of P2X receptors and ATP signalling at synapses. *Nat. Rev. Neurosci*. 2:165–174.

9. Khakh, B. S., and R. A. North. 2006. P2X receptors as cell-surface ATP sensors in health and disease. *Nature*. 442:527–532.

10. Torres, G. E., T. M. Egan, and M. M. Voigt. 1999. Hetero-oligomeric assembly of P2X receptor subunits. Specificities exist with regard to possible partners. *J. Biol. Chem*. 274:6653–6659.

11. Egan, T. M., and B. S. Khakh. 2004. Contribution of calcium ions to P2X channel responses. *J. Neurosci*. 24:3413–3420.

12. Jiang, L.-H., M. Kim, V. Spelta, X. Bo, A. Surprenant, and R. A. North. 2003. Subunit arrangement in P2X receptors. *J. Neurosci*. 23: 8903–8910.

13. King, B. F., A. Townsend-Nicholson, S. S. Wildman, T. Thomas, K. M. Spyer, and G. Burnstock. 2000. Coexpression of rat $P2X_2$ and $P2X_6$ subunits in Xenopus oocytes. *J. Neurosci*. 20:4871–4877.

14. Barrera, N. P., S. J. Ormond, R. M. Henderson, R. D. Murrell-Lagnado, and J. M. Edwardson. 2005. Atomic force microscopy imaging demonstrates that $P2X_2$ receptors are trimers but that $P2X_6$ receptor subunits do not oligomerize. *J. Biol. Chem*. 280:10759–10765.

15. Ormond, S. J., N. P. Barrera, O. S. Qureshi, R. M. Henderson, J. M. Edwardson, and R. D. Murrell-Lagnado. 2006. An uncharged region within the N terminus of the $P2X_6$ receptor inhibits its assembly and exit from the endoplasmic reticulum. *Mol. Pharm*. 69:1692–1700.

16. Collo, G., R. A. North, E. Kawashima, E. Merlo-Pich, S. Neidhart, A. Surprenant, and G. Buell. 1996. Cloning of $P2X_5$ and $P2X_6$ receptors and the distribution and properties of an extended family of ATP-gated ion channels. *J. Neurosci*. 16:2495–2507.

17. Rubio, M. E., and F. Soto. 2001. Distinct localization of P2X receptors at excitatory postsynaptic specializations. *J. Neurosci*. 21:641–653.

18. Schneider, S. W., J. Lärmer, R. M. Henderson, and H. Oberleithner. 1998. Molecular weights of individual proteins correlate with molecular volumes measured by atomic force microscopy. *Pflügers Arch*. 435:362–367.

19. Bobanovic, L. K., S. J. Royle, and R. D. Murrell-Lagnado. 2002. P2X receptor trafficking in neurons is subunit specific. *J. Neurosci*. 22: 4814–4824.

20. Soto, F., M. Garcia-Guzman, C. Karschin, and W. Stuhmer. 1996. Cloning and tissue distribution of a novel P2X receptor from rat brain. *Biochem. Biophys. Res. Commun*. 223:456–460.

21. Glass, R., A. Loesch, P. Bodin, and G. Burnstock. 2002. $P2X_4$ and $P2X_6$ receptors associate with VE-cadherin in human endothelial cells. *Cell. Mol. Life Sci*. 59:870–881.

22. Karlin, A., E. Holtzman, N. Yodh, P. Lobel, J. Wall, and J. Hainfeld. 1983. The arrangement of the subunits of the acetylcholine receptor of *Torpedo californica*. *J. Biol. Chem*. 258:6678–6681.

23. Gorrie, G. H., Y. Vallis, A. Stephenson, J. Whitfield, B. Browning, T. G. Smart, and S. J. Moss. 1997. Assembly of $GABA_A$ receptors composed of $\alpha1$ and $\beta2$ subunits in both cultured neurons and fibroblasts. *J. Neurosci*. 17:6587–6596.

24. Baur, R., F. Minier, and E. Sigel. 2006. A $GABA_A$ receptor of defined subunit composition and positioning: concatenation of five subunits. *FEBS Lett*. 580:1616–1620.

25. Aschrafi, A., S. Sadtler, C. Niculescu, J. Rettinger, and G. Schmalzing. 2004. Trimeric architecture of homomeric $P2X_2$ and heteromeric $P2X_{1+2}$ receptor subtypes. *J. Mol. Biol*. 342:333–343.

26. Nicke, A., H. G. Bäumert, J. Rettinger, A. Eichele, G. Lambrecht, E. Mutschler, and G. Schmalzing. 1998. $P2X_1$ and $P2X_3$ receptors form stable trimers: a novel structural motif of ligand-gated ion channels. *EMBO J*. 17:3016–3028.

27. Chu, Y., M. F. Mouat, J. A. Coffield, R. Orlando, and A. Grider. 2003. Expression of $P2X_6$, a purinergic receptor subunit, is affected by dietary zinc deficiency in rat hippocampus. *Biol. Trace Elem. Res*. 91:77–87.

28. Nawa, G., Y. Miyoshi, H. Yoshikawa, T. Ochi, and Y. Nakamura. 1999. Frequent loss of expression or aberrant alternative splicing of P2XM, a p53-inducible gene, in soft-tissue tumours. *Br. J. Cancer*. 80:1185–1189.

29. Park, H. C., J. Seong, J. H. An, J. Kim, U. J. Kim, and B. W. Lee. 2005. Alteration of cancer pain-related signals by radiation: proteomic analysis in an animal model with cancer bone invasion. *Int. J. Radiat. Oncol. Biol. Phys*. 61:1523–1534.

30. Urano, T., H. Nishimori, H. Han, T. Furuhata, Y. Kimura, Y. Nakamura, and T. Tokino. 1997. Cloning of P2XM, a novel human P2X receptor gene regulated by p53. *Cancer Res*. 57:3281–3287.